PERFORMANCE OF SMALL-SCALE FREQUENCY REFERENCES

J. Kitching[1], S. Knappe[2] and L. Hollberg[2]

[1]Time and Frequency Divison, NIST and JILA

[2]Time and Frequency Division, NIST, M.S. 847.10, 325 Broadway, Boulder, CO 80305-3328

Abstract – We consider theoretically the expected performance of ultra-small vapor-cell frequency references with cell volumes below 1 mm³. The short-term stability is found to degrade as the size is reduced. The amount of degradation depends on whether a buffer gas or wall coating is used for the atomic confinement. Preliminary experimental results with all-optical excitation indicate that the atomic Q-factor behaves as expected.

Keywords - Atomic clock, buffer gas, coherent population trapping, dark line resonance, vapor cell frequency reference, wall coating,.

I. INTRODUCTION

In this article, we analyze theoretically, the fundamental limits to the performance of small-scale frequency references as a function of the vapor cell's size. Ultra-small atomic frequency references, with dimensions of the order of 1 cm³ or below, are currently attracting significant attention because of their high potential for use in both commercial [1] and military [2] applications. The current generation of commercially available compact frequency references typically have a total volume of ~ 100 cm³, a physics package volume of ~ 1 cm³, and a weight of 250 g, and dissipate ~ 1 W of electrical power. Most of these references are lamp-pumped, vapor-cell designs, with cell volumes > 0.1 cm³.

Further miniaturization of vapor-cell frequency references must address a number of both fundamental and technical issues. These issues include: the fabrication of ultra-small vapor cells; the integration of optical components such as the photodetector and optical source, the size of the microwave cavity, the size of the control electronics, the power required to thermally control the physics package, and the size and power dissipation of the local oscillator and RF synthesis chain.

All-optical excitation techniques [3,4,5,6] have shown promise for simplifying the design of both compact frequency references [7] and magnetometers [8]. This novel excitation method relies on the nonlinear properties of atomic systems to carry out the hyperfine excitation of the atomic resonance. In conventional designs, the "clock" transition between the atomic ground-state hyperfine levels is excited using an oscillating magnetic field applied to the atoms by placing the vapor cell inside a microwave cavity connected to a microwave source. This oscillating magnetic field directly couples the hyperfine levels and thereby excites the coherence. In the all-optical method, microwaves are not applied directly to the atoms. Instead, two optical fields separated in frequency by the ground-state hyperfine splitting of the atoms are sent through the sample. The hyperfine coherence is created by the "mixing" of the optical

fields by the nonlinearity of the atom. The oscillating magnetic moment corresponding to the hyperfine coherence can be detected directly by means of a microwave cavity [9]. Alternatively, the change in light absorption when the difference between the optical frequencies is near the atomic hyperfine splitting can be measured. In our experiments [10], the two optical fields are created by modulating the injection current of a diode laser. Modulation at the first subharmonic of the atomic hyperfine splitting, for example, produces two first-order sidebands that can be simultaneously resonant with the optical transitions from each of the ground-state hyperfine levels. These two sidebands then form the Λ-system necessary for the all-optical excitation. When the modulation frequency is near the atomic hyperfine splitting frequency, the changing optical absorption of the atoms can be used to correct the modulation frequency and lock the modulation source to the atomic transition. A simple diagram outlining this technique is shown in Figure 1.
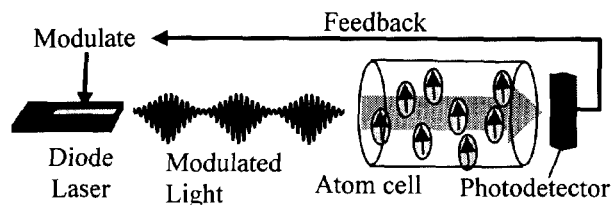

Figure 1. Schematic of the all-optical excitation method for a vapor-cell frequency reference.

The success of this all-optical excitation in previous experiments, particularly with regard to miniaturization, motivates the consideration of extremely small vapor-cell atomic frequency references. The primary performance figure we consider is the short-term frequency stability as determined by the Allan deviation, although some analysis is also offered regarding the long-term stability. Finally, we present some preliminary experimental results that support the theoretical analysis.

II. THEORETICAL ANALYSIS

The size of the vapor cell used to confine the atomic system affects the short-term stability in several ways. It changes the atomic transition width since atoms interact with the walls of the cell, alters the transmitted optical power through the cell, and determines the total number of atoms interacting with the optical field. We proceed by evaluating theoretically the short-term frequency instability, as determined by the Allan deviation. The Allan deviation is given in terms of the

atomic resonance Q-factor and detection signal-to-noise ratio, S/N, as [11]

$$\sigma_y = \frac{\chi}{Q(S/N)\sqrt{\tau}},$$ (1)

where τ is the integration time and χ is a parameter of order unity related to the method of interrogation of the resonance signal. The goal, then, is to determine the Q-factor and signal-to-noise ratio for the frequency reference as a function of cell size, for transitions narrowed with either buffer gas or wall coating.

When a buffer gas is used, the frequency width of the atomic microwave resonance is determined by both collisions with the buffer-gas atoms and diffusion to the cell walls. If the cell's dimension is much larger than the mean-free-path of alkali atoms in the buffer gas, the atomic Q-factor is related to the lowest-order diffusion mode and is given by [12]

$$Q_{bg} = \frac{f_0}{\Delta f_{bg}} = \frac{\pi f_0}{\gamma_k + \frac{D\xi^2}{R^2}},$$ (2)

where f_0 is the resonance frequency, Δf_{bg} is the full-width-at-half-maximum (FWHM) of the transition, γ_k is the coherence decay rate due to collisions with the buffer-gas atoms, assumed to be much larger than the radiative decay rate, D is the diffusion constant of the alkali atoms in the buffer gas, R is the cell size, and ξ is a constant of order unity related to the geometry. For the relevant range of operating conditions, γ_k and D are respectively directly and inversely proportional to the buffer-gas pressure. When a wall coating, rather than a buffer gas, is used to narrow the resonance width, the atomic Q-factor becomes [12]

$$Q_{wc} = \frac{\pi f_0}{\zeta \alpha_k \bar{v}} R,$$ (3)

where ζ is another geometrical constant of order unity, $\bar{v}$ is the mean atom velocity, and α_k is the probability of hyperfine decoherence for an atom upon collision with a cell wall. For glass surfaces, $\alpha_k \sim 1$, while for advanced wall coatings such as paraffin or tetracontane, $\alpha_k \sim 0.002$. It has been assumed for simplicity in both the buffer-gas and wall-coated cases that the entire cell is illuminated by the optical pumping light. Q-factors as a function of cell size for typical parameter values are show in Figure 2. The intrinsic Q-factor of the atoms is therefore given by either Eq. (2) or (3), depending on whether a buffer gas or wall coating is used for the confinement.

The intrinsic Q-factors in Eqs. (2) and (3) are reduced by two additional effects: spin-exchange collisions between alkali atoms [12], and power broadening by the optical field used to pump the atomic system [11]. These effects can be included as

$$\frac{1}{Q_{tot}} = \frac{1}{Q_{int}} + Bn_{alkali} + CI_{opt},$$ (4)

where Q_{int} is given by either Eq. (2) or Eq. (3), n_{alkali} is the number density of alkali atoms, I_{opt} is the incident optical intensity, and B and C are constants.

We next estimate the maximum detection signal-to-noise ratio. If the detected signal is proportional to the absorbed optical intensity, it can then be written $S=\beta I_{opt}A(\alpha L)$, where β is the fractional change in atomic absorption when the microwave frequency is brought into resonance with the atomic transition, $A=\pi R^2$ is the cross-sectional area of the light beam, α is the absorption coefficient of the atoms, and L is the length of the cell; it has been assumed that the cell is optically thin. Assuming shot-noise-limited detection, the noise spectral density is given by [13]: $N^2 = 2h\nu P_{trans} = 2h\nu I_{opt}A(1-\alpha L)$, where P_{trans} is the power transmitted through the cell, and $h\nu$ is the energy of one optical photon.
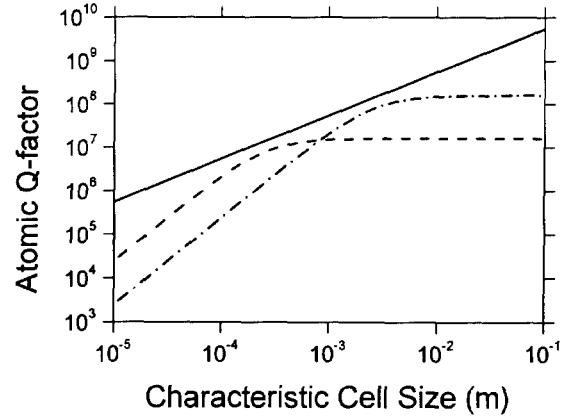

Figure 2. Atomic Q-factors as a function of cell size for a wall-coated cell with $\alpha_k=0.002$ (solid line); a buffer-gas cell with 100 kPa N_2 (dashed line); and a buffer-gas cell with 10 kPa N_2 (dot-dashed line).
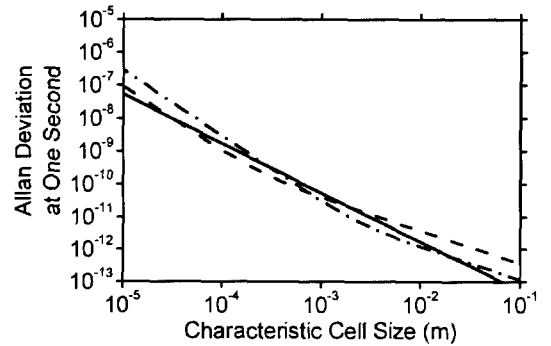

Figure 3. Optimum Allan deviation as a function of cell size for a wall-coated cell with $\alpha_k=0.002$ (solid line); a buffer-gas cell with 100 kPa N_2 (dashed line); and a buffer-gas cell with 10 kPa N_2 (dot-dashed line).

The expressions for the signal and noise can then be combined with Eqs. (4) and (1) to obtain an expression for the Allan deviation that is a function of the two main configurational parameters, n_{alkali} and I_{opt}. For a given cell size, the Allan deviation can be optimized with respect to these two parameters. We take n_{alkali} to be such that the optical thickness of the atomic sample is a constant, w, independent of length, L: $n_{alkali} = w/(\sigma_{abs}L)$. Here σ_{abs} is the cross-section for absorption of light by the atoms. It is then straightforward to find an optimum value for I_{opt}. The final result for the optimized Allan deviation, as a function of cell size, is

$$\sigma_y^{(opt)} = \frac{2\sqrt{2\chi}}{\sqrt{\pi}\beta w\sqrt{\tau}}\sqrt{h\nu C}\frac{1}{R}\sqrt{\frac{1}{Q_{int}} + \frac{Bw}{\sigma_{abs}L}} \ . \qquad (5)$$

With the use of the expressions for the intrinsic Q-factors, Q_{int}, for transition widths narrowed by a buffer gas (Eq. (2)) and wall coating (Eq. (3)), the optimized Allan deviation is plotted as a function of cell size (for R=L) in Figure 3. The curves in this figure assume a resonance contrast (β, defined as the ratio of the change in absorption on-resonance to the total absorption off-resonance) of 10 %, an optical absorption, w, of 10 % and parameter values $\chi=1$, B = 3.7 × 10^{-20} cm^3, C_{bg} = 7.3 × 10^{-9}/(μW/cm^2) and C_{wc} = 1.5 × 10^{-7}/(μW/cm^2). The values for C are not particularly well known and are estimated from a variety of previously published results. It can be seen that buffer-gas cells and wall-coated cells perform comparably over a wide range of cell sizes. The change in slope for the buffer-gas curve near R = 2 mm is related to the change in dominant decoherence mechanism from collisions with cell walls (at small cell dimensions) to collisions with buffer-gas atoms (at large cell dimensions). For a constant buffer-gas pressure, frequency references based on buffer-gas cells have performance inferior to those based on wall-coated cells at very small length scales because of the increasing surface-to-volume ratio. In small cells, the hyperfine decoherence of atoms in a buffer-gas cell becomes dominated by interactions with the (uncoated) walls, which reduce the Q-factor significantly more than occurs in a wall-coated cell.

A final important consideration is that of the AC Stark shifts that will be present while the system is operating. These shifts occur because the optical field used to excite the resonance also shifts the atomic levels. Primarily, we are concerned here with the extent to which these shifts affect the long-term stability of the frequency reference. In order to evaluate these shifts, we evaluate the optical intensity required to give the optimum short-term stability of Eq. (5). This optimum intensity is roughly that for which the power broadening of the microwave transition is equal to the intrinsic width of the transition added to the broadening due to the alkali-alkali collisions. This intensity can be written:

$$I_{opt} = \frac{1}{CQ_{int}} + \frac{B}{C}n_{alkali} \ , \qquad (6)$$

where Q_{int} is the intrinsic Q-factor given by either Eq. (2) or Eq. (3).

The AC Stark shift is nominally proportional to the optical intensity. For free Cs atoms (in a wall-coated cell, for example), the constant of proportionality is determined by the natural linewidth of the optical transition and is of the order of [14]

$$\frac{\Delta f_{Stark}^{(wc)}}{f} \approx \frac{5 \times 10^{-10}}{\mu W / cm^2} I_{opt} \ . \qquad (7)$$

For Cs atoms in a buffer-gas, the Stark shift is smaller [14] for a given optical intensity due to collisions of the alkali atoms with the buffer gas atoms, which reduce the optical transition probability:

$$\frac{\Delta f_{Stark}^{(bg)}}{f} \approx \frac{4 \times 10^{-12}}{\mu W / cm^2} \left(\frac{100 kPa}{P}\right) I_{opt} \ , \qquad (8)$$

where P is the pressure of the buffer gas. Fractional Stark shifts are plotted as a function of the characteristic cell
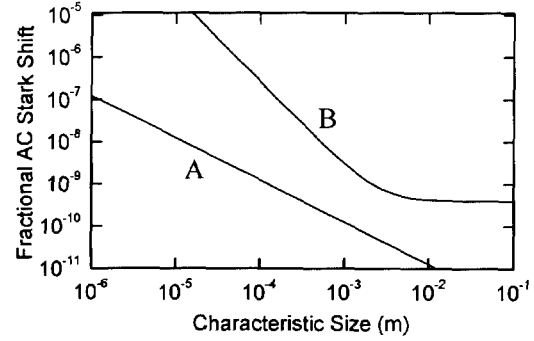

Figure 4. Fractional AC Stark shifts corresponding to the optical intensities used to achieve the short-term stability shown in Figure 3 for a wall-coated cell (Trace A) and a cell with a buffer gas of 10 kPa N_2 (Trace B).

size in Figure 4, where a buffer-gas pressure of 10 kPa has been assumed. It can be seen that the wall-coated cell is expected to perform somewhat better than the buffer-gas cell in this regard, mainly because the optical intensities required to optimize the short-term stability are considerably smaller. When the atoms are excited using a modulated laser field, substantially reduced AC Stark shifts are possible because of multiple optical sidebands generated by modulation of the laser [15].

Figure 4 indicates that for a millimeter-scale buffer-gas cell, the optical intensity would need to be stabilized to roughly 0.1 % in order to achieve a long-term fractional frequency stability of 10^{-11}. Such a level of intensity stabilization appears feasible with active control of laser power. Somewhat less power stability would be required to obtain the same long-term fractional frequency stability for a wall-coated cell. It should be noted, however, that while the scaling in Figure 4 is easily understood, the exact values of

the shifts these curves predict depend on the rather poorly known parameters C and Δf_{Stark}.

III. PRELIMINARY EXPERIMENTAL RESULTS

Initial experiments observing dark line resonances in small dimension cells supported the theoretical analysis above. Measurements of dark-line resonances were made on vapor cells ~ 1 mm thick (with large diameter) containing Cs vapor in a N_2 buffer gas. The cells were heated to ~ 50 °C, and magnetically shielded with high-permeability material, and the CPT resonance was observed by transmitting a modulated laser beam through the cell. The change in transmitted power, normalized to the Doppler absorption profile, is shown in Figure 5 for a cell with 21 kPa of buffer gas. The resonance in this case is roughly 500 Hz wide (at 9.2 GHz) and the contrast is about 0.2 %. While the observed contrast is substantially smaller than has been observed with larger cells (~ 1-2 % for D_2-line excitation), it is unclear at present whether this is due simply to the low optical intensity or high buffer-gas pressure used for this particular experiment. Other measurements we have made in cylindrical cells 2 mm in diameter show resonance contrasts comparable to those for centimeter-scale cells with sufficient intensity.
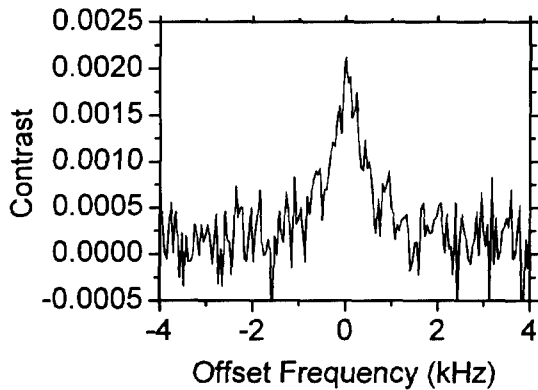
Figure 5. A CPT resonance observed in a 1 mm-long cell with 21 kPa of N_2 as a buffer gas.

A plot of the resonance Q-factor as a function of buffer-gas pressure for a 1 mm-long cell is shown in Figure 6. The solid line is a calculation based on Eq. (2) with values of the hyperfine decoherence cross-section and diffusion constant of $\sigma_{N2} = 3 \times 10^{-21}$ cm^2 and $D_0 = 0.12$ cm^2/s. For this size cell, the buffer-gas pressure required to optimize the atomic Q-factor is about 25 kPa.

IV. CONCLUSION

We have presented a theoretical analysis of the expected performance of vapor-cell frequency references as a function of cell size. This analysis indicates that for shot-noise-limited detection and resonance contrast of 10 %, a stability of

below 10^{-10} could be achieved at an integration time of one second. Furthermore, if the optical intensity were stable over the long term to 0.1 %, it is anticipated that the long-term frequency drift due to the AC Stark shift would be near 10^{-11}. Initial measurements on the linewidth of CPT resonances in millimeter-scale cells seem to support the theoretical treatment.
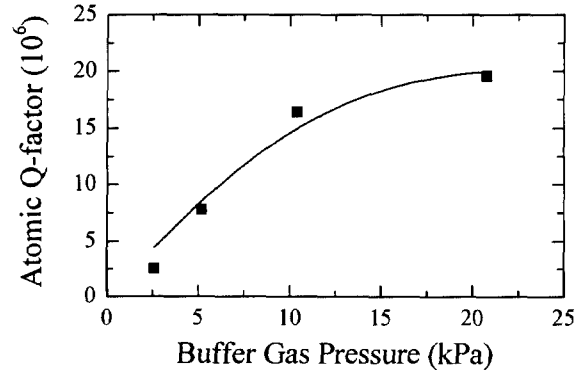
Figure 6. The atomic Q-factor for a 1 mm-long cell as a function of the pressure of the N_2 buffer gas.

REFERENCES

[1] J. Kusters, "Performance requirements of communications base station time standards", RF Design, May, 1999.
[2] J. R. Vig, "Military applications of high accuracy frequency standards and clocks," IEEE Trans. Ultra. Ferr. Freq. Control, vol. 40, pp. 522,1993.
[3] E. Arimondo, "Coherent population trapping in laser spectroscopy," in Progress in Optics XXXV, E. Wolf, ed., Elsevier Science B.V., 1996, pp. 257-354.
[4] J. E. Thomas, S. Ezekiel, C. C. Leiby, Jr., R. H. Picard, and C. R. Willis, "Ultrahigh resolution spectroscopy and frequency standards in the microwave and far-infrared regions using optical lasers," Opt. Lett., vol. 6, pp. 298-300, 1981.
[5] A. M. Akulshin, A. A. Celikov and V. L. Velishanski, "Sub-natural absorption resonances on the D_1 line of rubidium induced by coherent population trapping," Opt. Comm., vol. 84, pp. 139-143, 1991.

[6] N. Cyr, M. Tetu and M. Breton, "All-optical microwave frequency standard: a proposal," IEEE Trans Instrum. Meas., vol. 42, pp. 640-649, 1993.

[7] J. Kitching, L. Hollberg, S. Knappe and R. Wynands, "Compact atomic clock based on coherent population trapping," Electon. Lett. Vol. 37, pp. 1449-1451, 2001.

[8] M. Stahler, S. Knappe, C. Affolderbach, W. Kemp and R. Wynands, "Picotesla magnetometry with coherent dark states," Europhys. Lett., vol. 54, pp. 323-328, 2001.

[9] A. Godone, F. Levi and J. Vanier, "Coherent microwave emission in cesium under coherent population trapping," Phys. Rev. A, vol. 59, pp. R21-R15, 1999.

[10] J. Kitching, S. Knappe, N. Vukicevic, L. Hollberg, R. Wynands and W. Weidemann, "A microwave frequency reference based on VCSEL-driven dark line resonance in Cs vapor," IEEE Trans. Instrum. Meas., vol. 49, pp. 1313-1317, 2000.

[11] J. Vanier and C. Audoin, "The Physics at Atomic Frequency References," Bristol: Adam-Hilger, 1989.

[12] W. Happer, "Optical pumping," Rev. Mod. Phys., vol. 44, pp. 169-242, 1972.

[13] A. Yariv, "Quantum Electronics," 3rd Ed., New York: Wiley, 1989.

[14] A. Nagel, S. Brandt, D. Meschede and R. Wynands, "Light shift of coherent population trapping resonances," Europhys. Lett., vol. 48, pp. 385-389, 1999.

[15] M. Zhu and L. S. Cutler, "Theoretical and experimental study of light shift in CPT-based Rb vapor cell frequency standard," Proc. 32nd Annual Conference on Precise Time and Time Interval Systems and Applications Meeting, Reston, VA, pp. 311-324, Nov. 2000.